Breaking focused wave interaction with cylinder using HOS-OpenFOAM coupling

Sithik Aliyar, Guillaume Ducrozet, Benjamin Bouscasse, Sriram Venkatachalam, Pierre Ferrant

Breaking focused wave interaction with cylinder using HOS-OpenFOAM coupling

Sithik Aliyar[a,b]
[a]Dept of Ocean engineering
Indian Institute of Technology, Madras
Tamil Nadu, India- 600036
ORCID: 0000-0003-0188-4613

Guillaume Ducrozet[b]
[b]LHEEA Res. Dept. (ECN and CNRS)
École Centrale de Nantes
44321 Nantes, France
guillaume.ducrozet@ec-nantes.fr

Benjamin Bouscasse[b]
[b]LHEEA Res. Dept. (ECN and CNRS)
École Centrale de Nantes
44321 Nantes, France
benjamin.bouscasse@ec-nantes.fr

Sriram Venkatachalam[a]
[a]Dept of Ocean engineering
Indian Institute of Technology, Madras
Tamil Nadu, India- 600036
vsriram@iitm.ac.in

Pierre Ferrant[b]
[b]LHEEA Res. Dept. (ECN and CNRS)
École Centrale de Nantes
44321 Nantes, France
pierre.ferrant@ec-nantes.fr

OCEANS 2022 - Chennai | 978-1-6654-1821-8/22/$31.00 ©2022 IEEE | DOI: 10.1109/OCEANSChennai45887.2022.9775539

***Abstract*—Extreme waves endanger offshore structures under severe environmental conditions. These large and steep waves are highly nonlinear, which can cause high-intensity and short-duration impact forces. It is vital to understand the impact created by such extreme events over any structure. The objective is to investigate wave impact forces on a vertical surface piercing cylinder subjected to breaking waves. The numerical simulation is carried out with a hybrid coupled solver named *foamStar*. It couples a High-Order Spectral (HOS) based nonlinear potential model and an OpenFOAM based CFD model.The HOS model describes accurately in a fully nonlinear potential flow framework the focused breaking wave without the structure. The CFD model is based on the incompressible Reynolds-averaged Navier–Stokes equations and the volume of fluid for the free surface. The coupled model is a CFD based numerical wave tank. First, the focused wave onset of breaking is validated in HOS-NWT and foamStar, and then its interaction with the cylinder is addressed. The experimental results used in this paper correspond to the experiments performed in Ludwig-Franzius-Institute, Germany[1]. The experimentally measured main wave crest of the breaking focused wave group with its total forces and pressure over a cylinder is fairly well captured in the numerical simulation. Further, the evolution of focused breaking waves along the tank and their characteristics were examined. An overall good degree of agreement is reported, which denotes that the model can be a helpful tool to evaluate breaking wave forces on structures.**

***Index Terms*—HOS, focusing wave, breaking wave, wave forces, wave impact, vertical cylinder, Computational Fluid Dynamics, OpenFOAM, foamStar**

I. Introduction

The coastal (Piers, Jetties, Berthing and Mooring structures) and offshore structures (Jacket, TLP, SPAR, semi-submersible, etc.) are generally made of cylindrical members, and are often exposed to severe waves. Their design primarily depends on such extreme forces that the structures would encounter in their life span. Much research has been carried out for decades on the accurate evaluation of wave forces. The estimation of wave force determination on cylinders depends on two parameters, cylinder diameter(D) to wavelength (λ) ratio ($\pi D/\lambda$) and Keulegan-Carpenter (KC) number [2]. The KC number is a ratio that measures the importance of inertial and drag forces. For $D/L < 0.2$ and $KC > 2$, wave forces on cylinders are generally determined using the Morison formula [3], which accounts for the inertial and drags component of the wave forces with empirical force coefficients. [4] modified the Morison equation with the impact force term to estimate total force from the breaking waves. There will be a very high magnitude of impact force in breaking waves acting over a short duration. The direct modelling of breaking waves is challenging due to the complex nature of the physical processes, including highly non-linear interactions. Researchers carried several experiments [4; 5; 6; 7] that led to a better understanding of the breaking wave forces. However, the accurate measurement of velocity and acceleration during the impact is still challenging. Also, above studies indicated that parameters that influence the breaking forces can be breaker type, the distance of the structure from the breaker location, the shallow water depth that induces breaking etc. In the complex case of breaking wave interaction, numerical simulations can be used to capture the flow field details that are challenging to measure in experimental studies due to various factors (cost, instrumentation and structural response, time-limit etc). Another advantage is that numerical simulation can control breaker locations, which is not easier to carry out in the experiments [8].

In shallow waters, waves deform as they propagate into decreasing water depth. The effects of the sea bottom and shoaling are included as additional terms in defining the breaking criteria. But in deep waters, it is always related to the physical properties of the highest steady wave, which limits the wave growth and causes breaking. Most numerical solvers develop breaking waves using a plane slope inside the domain, resembling the breaking phenomenon in shallow water waves.

But another way of generating breaking waves is using the dispersive focused wave breaking near the structure as adopted in [9]. This type of wave-wave interaction allows the control of the breaking events' location. Hence, different types of breaking load on the structure can be generated by adjusting the focusing point. The latter type of breaking wave generation is adopted in the current study.

The numerical modelling of breaking waves involves models based on Boussinesq equations, Potential theory and Navier-Stokes equation (CFD approach). The Boussinesq wave model is based on depth-averaged equations with dispersive terms and may be more accurate for describing the wave transformation in shallow waters. However, the application of this type of model is confined to the region before breaking, and it can not be directly used to represent the underlying physics of the breaking process due to the approximations involved in the modelling [10]. The recent developments in the Potential flow models can be used to model the breaking onset, including wave kinematics and pressure. But it can not be used to model the interface reconnection and the associated free surface deformation beyond the breaking point. Hence the breaking wave investigation is commonly solved using the Computational Fluid Dynamics (CFD) approach since it can accurately model the (pre-and) post-breaking kinematics marked by large vorticity and strong viscous dissipation comparison to other solvers. A considerable amount of work in generating breaking waves in CFD has been achieved in recent years [11], [12]. Although the CFD model can provide high-fidelity results, increased computational costs cannot be evaded. Hence the objective is to couple the potential flow models with the CFD model, combining the advantages of each method under domain decomposition (DD) approach [13]. It means, the complex interaction only appears in the vicinity of the structure and in the far-field, the viscous effects can often be neglected. Hence, splitting the computational domain into a viscous inner sub-domain and an inviscid outer sub-domain and solved with viscous CFD solver and potential flow solver, respectively. Simililar research were attempted to model two-dimensional breaking and post-breaking stages of solitary waves by combining the fully non-linear potential equations with the volume of fluid approach (VOF) [14; 15]. They demonstrated that the model is capable of simulating the flow features even after the overturning wave crest impinges the free surface. However, the model was not verified against experimental data.

In the present study, under the DD approach the OpenFOAM based solver *foamStar* [16] is coupled with potential flow model *HOS* [17] to replicate the focused breaking wave interaction with the slender cylinder. The model has been previously used to simulate the non-breaking wave cases and other applications [18; 19]. This is a new study investigating the breaking wave model implemented in *HOS-NWT* [20; 21] that is assessed within the *foamStar-HOS* coupled domain. The main advantage of using this coupling model instead of the pure CFD model is that the viscous domain is provided only near the structure, saving the prohibitive computational cost and avoiding the numerical damping in the wave propagation [13]. The experiments performed at the Franzius-Institute at Leibniz University of Hannover, Germany reported in [1] are used for validating the numerical model.

This paper presents the focused breaking wave interaction with the vertical cylinder in the following sections. Section 2 presents the numerical models with its description and Section 3 presents the validation of the focusing wave. In the first part of this section, the wave generated in the HOS-NWT is validated with the experimental results, and in the second part same HOS wave is passed through the CFD domain and mesh and time convergence study is carried out. In Section 4 the interaction study with the cylinder and its validation with the experiment is presented.

NUMERICAL MODEL

In the current research, one-way domain decomposition [13] using *foamStar* as the CFD solver and HOS-NWT as the potential solver is adopted. This section defines the governing equations behind the foamStar solver and its free surface capturing technique first, followed by HOS-NWT with its breaking model. Finally, the coupling between the foamStar solver and HOS-NWT is presented briefly.

foamStar

The foamStar is an in-house code co-developed by Bureau Veritas and Ecole Centrale de Nantes in the OpenFOAM framework for solving wave-structure interaction problems. It is based on the open-source solver interDymFoam solving the multiphase problem by coupling the Navier-Stokes equations with a Volume of Fluid (VoF) method [22]. The computational domain is subdivided into a finite number of control volumes(CV), which can be arbitrary. The integrals over each CV are numerically approximated using the midpoint rule. The pressure Poisson equation is solved based on a PIMPLE algorithm, which combines the Semi-Implicit Pressure Linked Equations (SIMPLE) algorithm with the Pressure Implicit with Splitting of Operators (PISO) algorithm. The unknown variables at the centre of a cell face are determined by combining a central differencing scheme (CDS) with an upwind differencing scheme (UDS). The governing equation for the Newtonian fluid are based on mass and momentum conservation equations written as follows,

$$\nabla.\boldsymbol{u} = 0 \tag{1}$$

$$\frac{\partial(\rho\boldsymbol{u})}{\partial t} + \nabla.(\rho\boldsymbol{u}\boldsymbol{u}^{\boldsymbol{T}}) - \nabla.[\mu(\nabla u + \nabla u^T)] = -\nabla p_d - (\boldsymbol{g}\cdot\boldsymbol{x})\nabla\rho \tag{2}$$

where $\boldsymbol{u}, \boldsymbol{x}$ and $\mathbf{g}$= $[0, 0, -g]^T$ are the fluid velocity, position vector and gravitational acceleration vector, respectively. The dynamic pressure $p_d = p - \rho\boldsymbol{g}\cdot\boldsymbol{x}$ is as introduced in [23]. The free surface is identified using the volume of fluid (VoF) method, where the two-phase problem is treated as a single fluid with a volume-fraction parameter $\alpha \in [0, 1]$ subjected to transport equation,

$$\frac{\partial \alpha}{\partial t} + \nabla.(\alpha \boldsymbol{u}) + c_\alpha \nabla.(\boldsymbol{u}_n \alpha(1-\alpha)) = 0 \tag{3}$$

where the third term on the left-hand-side is the artificial compression to keep the interface sharp. $\boldsymbol{u}_n$ is the fluid velocity normal to the interface and c_α is the compression coefficient. In each cell, then fluid properties (density and viscosity) are computed as a mixture between air ($\alpha = 0$) and water ($\alpha = 1$):

$$\rho = \alpha\rho_w + (1-\alpha)\rho_a \qquad \mu = \alpha\mu_w + (1-\alpha)\mu_a \tag{4}$$

where index w and a indicate water and air respectively.

HOS - Wave generation and modeling

The incident wave generation is based on the potential theory approach. With the assumption of ideal fluid and irrotational flow, it is possible to define a velocity potential(ϕ) as,

$$\boldsymbol{u}_I = \nabla\phi \tag{5}$$

Then the incident wave potential satisfies Laplace's equation in the fluid domain (Ω)

$$\Delta\phi = 0 \quad x \in \Omega \tag{6}$$

The dynamic and kinematic free surface conditions are expressed with η and $\tilde{\phi}$ as the free surface elevation and surface velocity potential is read as,

$$\frac{\partial \eta}{\partial t} = \left(1 + |\nabla\eta|^2\right)\frac{\partial \phi}{\partial z} - \nabla\tilde{\phi}\cdot\nabla\eta \tag{7}$$

$$\frac{\partial \tilde{\phi}}{\partial z} = -g\eta - \frac{1}{2}|\nabla\tilde{\phi}|^2 + \frac{1}{2}\left(1 + |\nabla\eta|^2\right)\left(\frac{\partial \phi}{\partial z}\right)^2 \tag{8}$$

The above unknown quantity is computed with the High-Order Spectral (HOS) method, using Taylor expansions and power series developments [24; 25]. Because of pseudo-spectral formalism, HOS exhibits high efficiency and accuracy, and it considers the complete non-linearity of the free surface. In this work, HOS-NWT(Numerical wave tank)[17], an open-source solver developed at LHEEA lab (Ecole Centrale Nantes), is used to solve the incident waves in NWT.

But the HOS-NWT model neglects vorticity and viscous phenomena, preventing the model's usage in breaking waves. A methodology has been recently implemented in HOS-NWT to take those breaking events into account [20; 21]. But to be noted that the breaking models implemented only emulate the wave spectrum modification due to breaking, dissipating energy in the relevant frequency range. The Tian-Barthelemy breaking model is used in this study and it is detailed in [26; 27]. A breaking onset criteria detects the breaking waves prior to their appearance. It is complemented by dissipative terms, introducing an eddy viscosity, added to the free surface boundary conditions following the Tian model. Definitions and recommended values for the model can be found in [20; 21; 26].

Relaxation Zone - Coupling between solvers

In general approach, generating a wave in the NWT is to mimic the paddle in the experimental tank as a moving boundary. However, the computational cost is prohibitive. The simplest way based on one way DD (*foamStar*) is to impose wave velocity and free surface elevation from potential wave models at the inlet zone of the CFD domain.An accurate and efficient interpolation method to map the results of HOS wave models onto the CFD mesh is made through solver Grid2Grid, an open-Source library [28]. In *foamStar*, the wave generation and absorption method are based on an explicit scheme that relaxes the computed solution towards a given target flow field [29],[30]). [31] can be referred for some examples of 3D wave generation of realistic sea spectrum.

COMPUTATIONAL DOMAIN

Experimental set up

The experiments performed in the Schneiderberg wave flume at Leibniz University of Hannover, Germany, by Sriram et al [1] are used in the present study. The laboratory measurements on focusing wave interactions on a similar setup with a fixed and moving cylinder have been released for a comparative study between different numerical models [32]. The tank is $110m$ long, $2.2m$ wide, and $2m$ deep. The flume was filled with fresh water to a working depth of $d = 0.7m$. The cylinder of interest is a $0.22m$ diameter, $12mm$ thick, and $L = 1.025m$ long aluminium cylinder. The variations in free-surface elevation along the tank are measured using seven resistance type wave gauges (WP1-WP7). WP1, which was placed close to the wavemaker ($x = 5.327m$), three-wave gauges (WP2-WP4) were placed at $x \approx 18m$ from the wavemaker. Other three-wave gauges (WP5-WP7) centred around $25m$ from the wave paddle, ie from the cylinder centre, WP5 is placed at $x = -0.555m$, WP6 is inline and WP7 placed at $x = +0.625m$ respectively. Typical representation of the probes and the experimental domain is as shown in the Figure 1

Apart from the wave-probes, eight pressure transducers were positioned over the surface of the cylinder to measure the time-varying and impulsive pressures induced by the waves. PP1-5 are placed at $0°$, facing the incident waves, at a uniform spacing of $0.1m$, with PP1 being the bottom most at a distance of $0.415m$ from the flume bottom. The three remaining transducers (PP6-8) are arranged at the same level as PP3 ($0.615m$ from the flume bottom) but circumferentially oriented at $20°$, $90°$ and $180°$. The total horizontal inline force on the cylinder was measured using a force transducer installed at the top bearing of the cylinder, which in turn rigidly fixed to the Steel frame in the flume. In the experiments, the wave elevation was sampled at $100Hz$ whilst the pressure and inline force were sampled at $9,600Hz$ to capture the extremely short-term impact pressures and loads induced by steep, breaking waves on the structure.

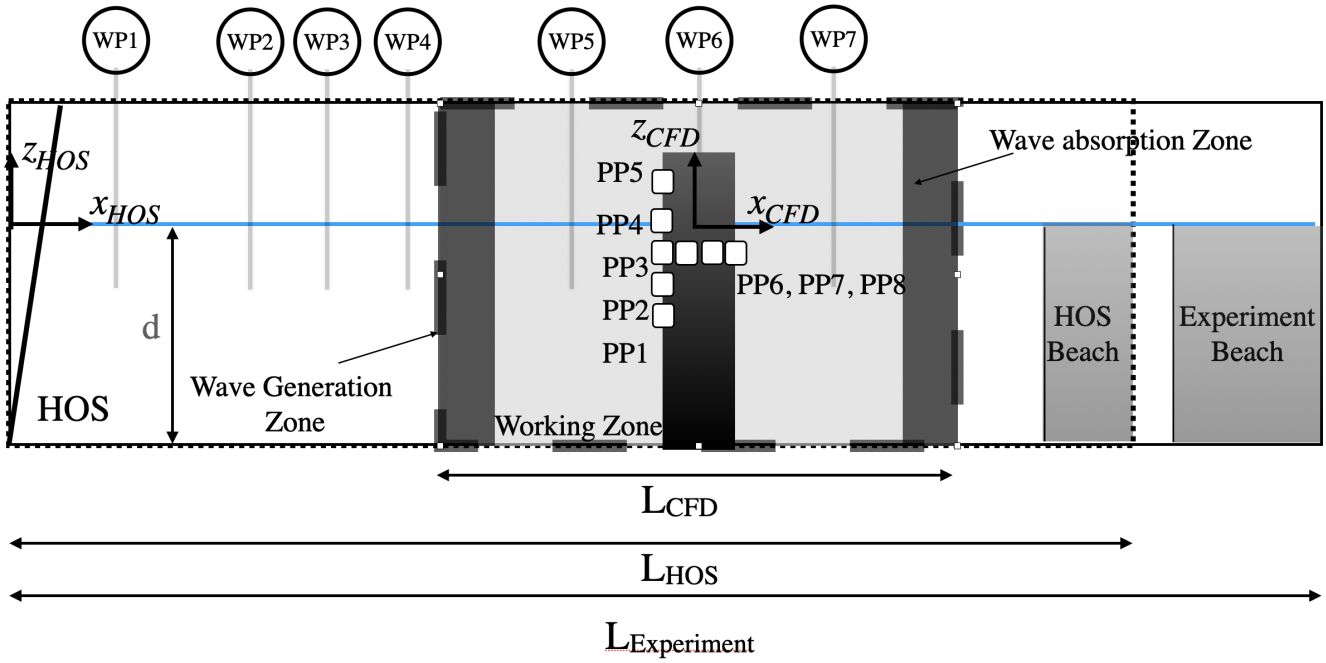

Fig. 1: Typical representation of the Experiment and Numerical wave tank of (*foamStar*) inside the HOS-NWT with wave probes(WP) and pressure sensors (PP)

Set up for Numerical simulation

The numerical domain reproduces the experimental configuration as shown in the Figure 1. Consequently, the computational domain for HOS is made similar to the experiment tank to reproduce the wave generation, propagation and absorption of waves. The HOS domain is chosen shorter than the experimental one since the structure is located at 25m, and we are not interested in happenings at the end of the tank (which is assumed not to have any influence on the results). The CFD zone (representing *foamStar* solver) is constructed around the cylinder, with its origin coinciding with the cylinder centre inside the HOS-NWT. The wave considered for validation is a unidirectional focusing wave group consisting of 32 wave components. The frequencies of the wave component's range from $f_l = 0.34$ Hz to $f_u = 1.02$ Hz with its central frequency at $f_c = 0.68$ Hz. The ratio of bandwidth to the central frequency is 1. The dimensions and probes of the numerical domain are identical to those of the wave flume mentioned in the experimental setup. N_x, the number of points in the domain controls the spatial discretization of the HOS-NWT. In the present study, the ratio of maximum wave number with wave number of central frequency (k_{max}/k_C) is maintained at 25, and the order of non-linearity of HOS is fixed to 5. The wave is generated by loading experimentally recorded wave paddle motion as input of HOS-NWT for a direct comparison to experiments, and the Tian model is used to account for the breaking waves. This 'classical' choice of parameters should ensure an accurate description of the wave field evolution in HOS-NWT. A constant phase shift observed in the experiment is of 0.14s[32]. This may be attributed to the trigger at use for the recording during experiments that possibly experienced such small time delay and this shift is corrected in the numerical results.

The wavelength of the particular central frequency (f_C) is $\lambda_c = 3.37$ m, which is used to fix the zonal lengths in the CFD. The wave generation, computational and wave absorption zones are fixed with a length of one λ, 1.5 λ and one λ, respectively. Two step procedures are being carried out, one for validating the wave without the structure(Two-dimensional NWT) and another validating wave structure interaction (Three-dimensional NWT). For the first case, Two dimensional NWT is made from the 3D tank by slicing a plane at the centre without the cylinder. For the second case, the CFD zone is made similar to experimental domain with the cylinder. Three wave probes WP5-7 fall in the zone with eight pressure probes identical to the experimental location. The force over the cylinder can be extracted using the OpenFOAM function objects to compare against the experimental force recordings.

RESULTS AND DISCUSSION

In this section, the validation of the hybrid coupling between HOS-NWT and *foamStar* is presented. This wave structure interaction study applies a two-step procedure. First, the focused breaking wave validation is given, and then the wave interaction with a vertical cylinder is demonstrated.

Focusing wave validation

This step consists of focusing wave propagation in a computational domain without the structure. Initially, HOS-NWT validation of the wave is presented, followed by *foamStar*

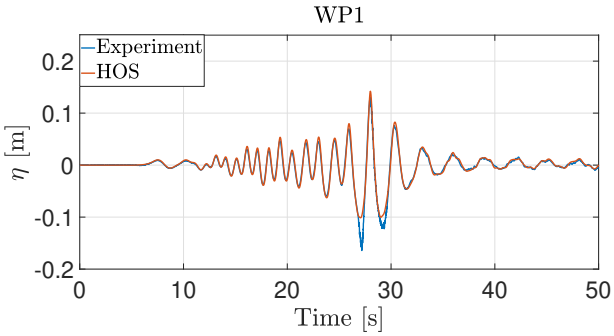

Fig. 2: Comparison of time series of the wave profile at near the paddle (WP1)

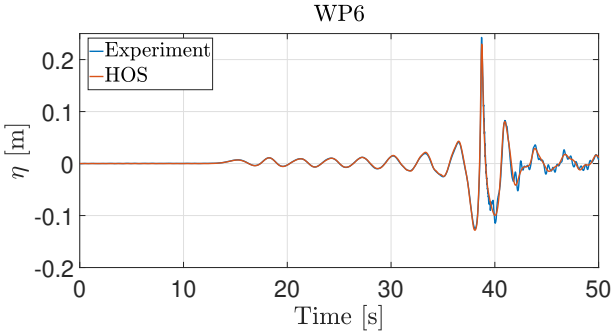

Fig. 3: Comparison of time series of the wave profile at near the paddle (WP1) and cylinder location (WP6)

confirmation. Different discretizations are used for the mesh and time convergence study to check whether a solver can generate accurate incident waves. A comparison with the experimental measurements is also provided.

HOS-NWT validation: The dimensions and probes of the numerical domain are identical to those of the wave flume mentioned in the experimental setup. The wave probe comparison at wave probe WP1 near the paddle and WP6 at the cylinder location are shown in the Figure 2 and Figure 3. Figure 2 shows overall excellent agreement, except in the two large troughs surrounding the largest wave. Figure 3 indicates very good agreement of the focused wave profile, including the preceding and following troughs. As expected, some discrepancies are observed after the breaking, which may be attributed to the breaking model that does not simulate the whole complexity of breaking waves (high-frequency waves observed after t=40s). The above outcome ensures an accurate and efficient solution to the problem, and this HOS wave elevation and velocity is provided at the inlet zone of the *foamStar* solver.

foamStar wave validation - Convergence study: The good quality of incident waves is the first requirement for any wave structure interaction problem. A mesh and time convergence study is carried out to reproduce the wave in the CFD zone. The simulations use a two-dimensional rectangular computational domain, and the waves travel from inlet to outlet. The length of the computational zone is fixed as 3.5λ ($1\lambda + 1.5\lambda + 1\lambda$) for the Mesh convergence study. Thirty combinations of mesh size and the time step are tried (see Table I) in terms of lateral spacing Δx, vertical spacing in the free surface zone Δz and time step Δt. The aspect ratio of cells in the free surface zone is maintained at 1. The number of cells per wavelength ($\Delta x/\lambda_C$) is varied from 32 to 1350, and for each case, five different Co are being tested. Representative cell-based Courant number can be defined by using analytic wave velocities [18],

$$Co = \sqrt{Co_x^2 + Co_z^2}$$

where

$$Co_x = \frac{u_{wave}\Delta t}{\Delta x}, Co_z = \frac{w_{wave}\Delta t}{\Delta z}$$

u_{wave} and w_{wave} are the maximum horizontal and vertical velocity (in this case 1.4 m/s and 0.5 m/s).

The overturning of the breaking wave occurs between the probe location WP5 and WP6. Hence the free surface elevation at the WP5, which is irrotational, is chosen for the validation study. Figure 4 plots the time series of surface elevation for the typical combinations of test cases from fs1 to fs6 mesh types for Co 0.1. The cross-correlation coefficient method is adopted for this comparison study as it has the advantage of measuring the similarity between the signals and the time shift between them. HOS wave probe results are used as a reference medium here for two reasons. First, there is a slight discrepancy in the experiment and HOS results that will be there in CFD. Second, the HOS wave is fed as an input condition in the CFD, making the HOS wave most appropriate to compare with the CFD results. Figure 5 represents the

TestCase Name	$\Delta x/\lambda_C$	Courant number (Co)
fsM1	32	1 0.75 0.5 0.25 0.1
fsM2	64	1 0.75 0.5 0.25 0.1
fsM3	128	1 0.75 0.5 0.25 0.1
fsM4	256	1 0.75 0.5 0.25 0.1
fsM5	338	1 0.75 0.5 0.25 0.1
fsM6	1350	1 0.75 0.5 0.25 0.1

TABLE I: Mesh and time discretization for the convergence tests. fs represents *foamStar* and M1 ... M6 represents coarser to finer mesh type

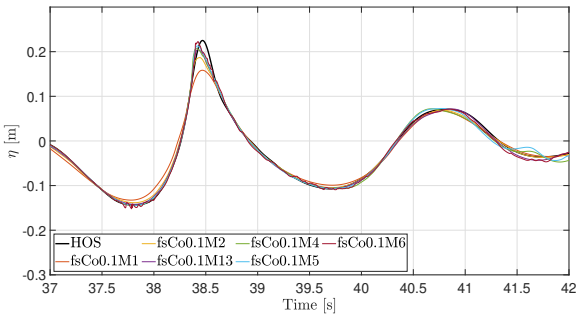

Fig. 4: Typical comparison of time series of the wave profile at (WP5) for test cases M1 to M6 with Co 0.1

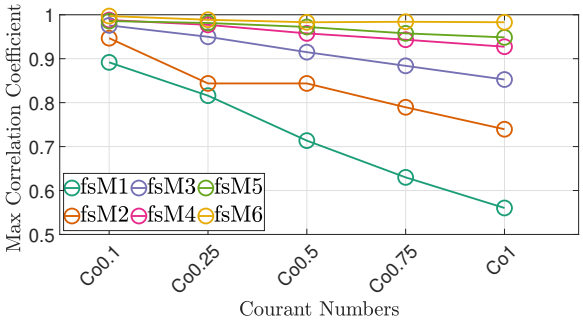

Fig. 5: Comparison of Cross correlation coefficient for the wave generated in the *foamStar* with HOS wave for different mesh types and Courant number

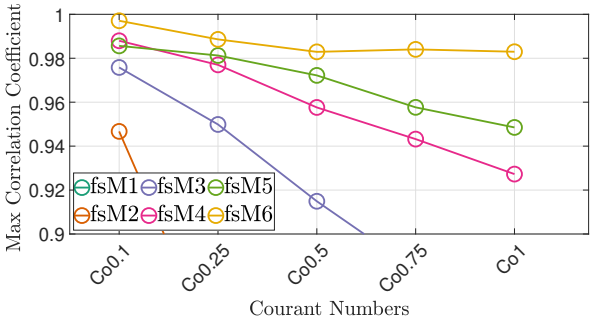

Fig. 6: Zoomed window of Figure 5

maximum of the cross-correlation coefficient as a function of Co for different mesh sizes (fs1 to fs6). Figure 6 illustrates the zoomed window to observe the minor changes in the previous Figure. The Figure shows that accuracy increases by refining the mesh and downsizing the Courant number for almost all the cases. The coarse mesh types (fsM1 and fsM2) showed good convergence when moving from Co 1 to Co 0.1, from 0.58 to 0.88 and 0.74 to 0.95, respectively. Attaining one (a perfect case) looks computationally expensive, seeing from the case of fsM6. Even the most refined mesh and finest time step (fsM6Co0.1)would reach an accuracy of only 0.995. In the present study, fsM4Co0.1 proves to be economical in terms of spatial and temporal resolution with an accuracy of more than 0.99 and hence chosen for the wave structure interaction study.

Focusing wave structure interaction

This section validates the model capability to measure the wave force, surface elevation, pressure over the cylinder and validated with the experimental results. The three-dimensional simulation of the focused wave structure interaction is performed with a vertical circular cylinder in a NWT. The interaction modifies the kinematics and the flow field around the cylinder as shown in Figure 7. To understand the Figure, a new parameter t_h is introduced, where it is the time at which wave hits the cylinder. This figure displays the free surface features with velocity magnitude when the focused wave interacts with the cylinder for different time instants. Figure 7a represents the wave reaches its maximum height and it is about to start curling.

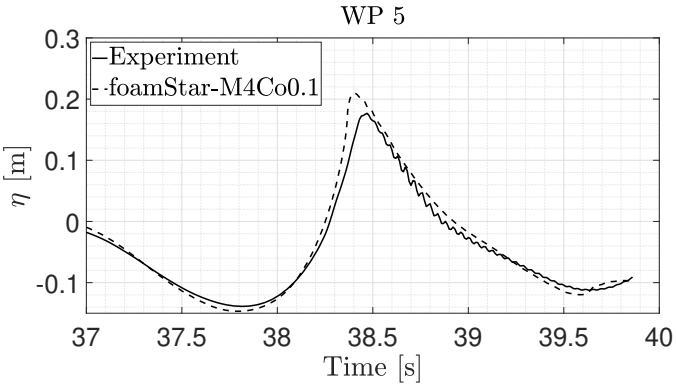

(a) Waveprobe WP5

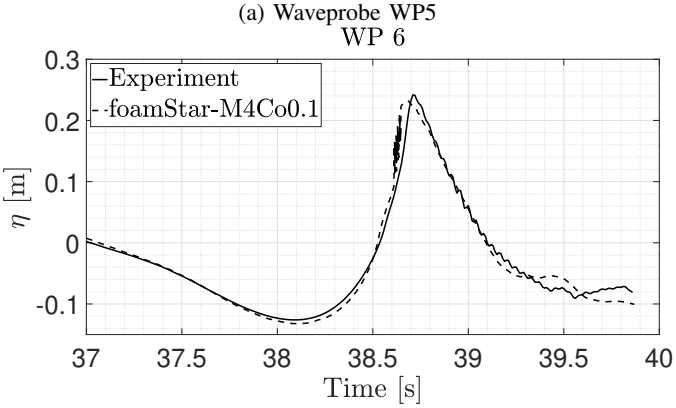

(b) Waveprobe WP6

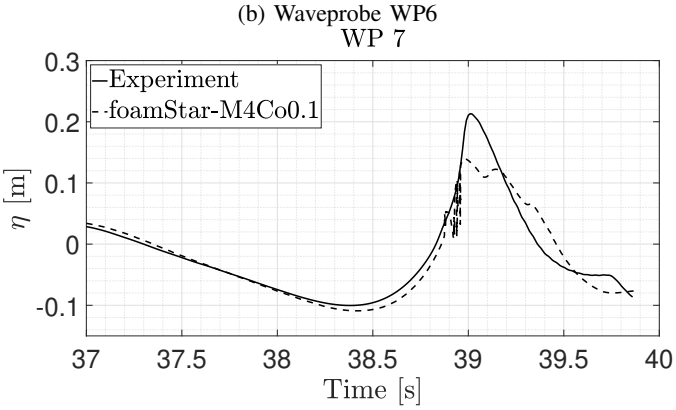

(c) Waveprobe WP7

Fig. 10: Illustration of Wave probe comparison between Mesh type fsM4Co0.1 of *foamStar* solver and Experiment

The highly curled wave crest impacts the cylinder much below the top wave crest level in Figure 7b. Figure 7c shows the separation of the incident wavefront and the formation of a semi-circular wavefront meeting behind the cylinder. The broken wave separated around the cylinder propagates further with a region of low velocity in the shadow region behind the cylinder. A mildly developed chute-like jet is seen in Figure 7d which is close to its collapse state, and this weakly developed chute wave is seen to rejoin the free surface at some

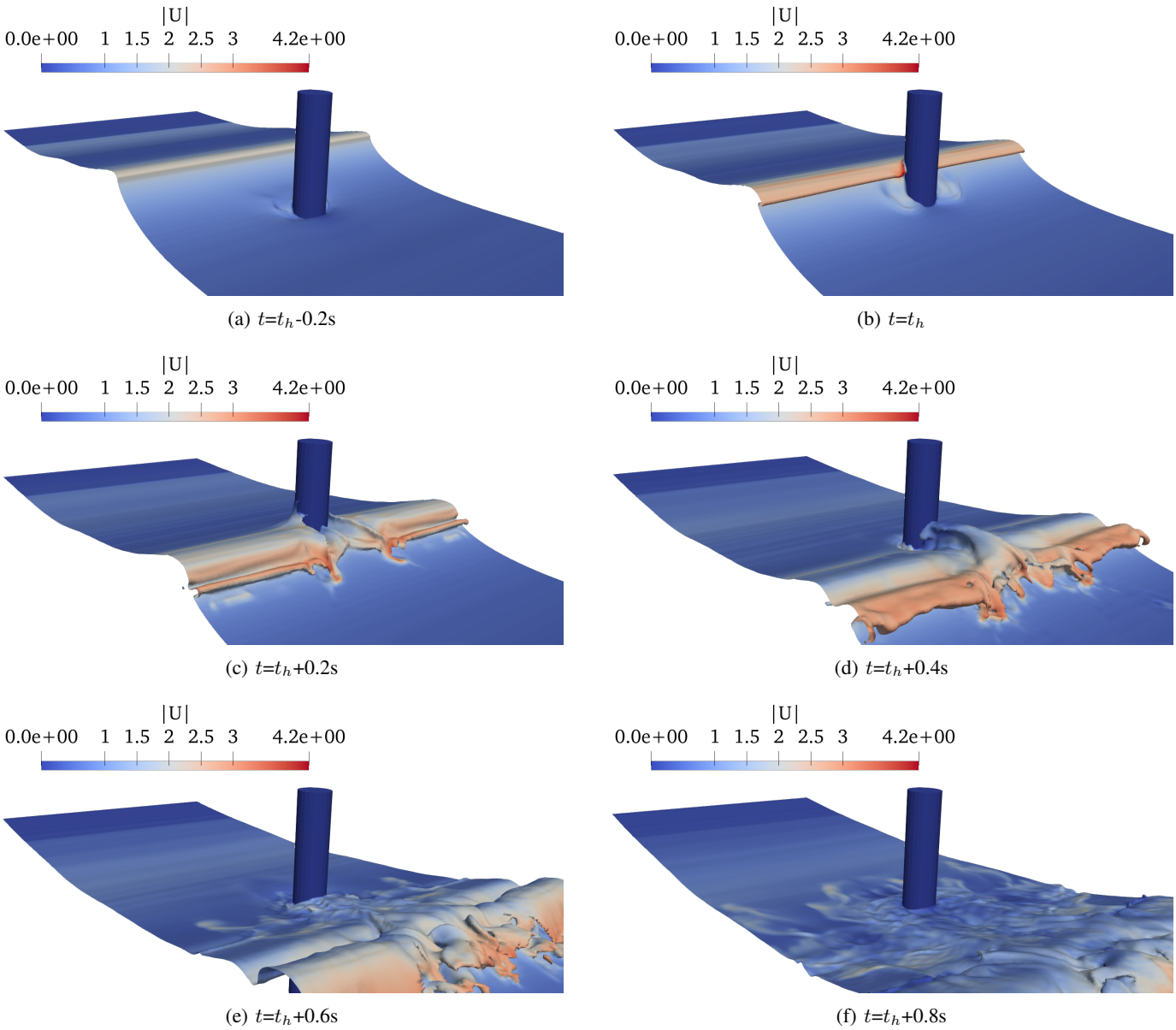

(a) t=t_h-0.2s (b) t=t_h

(c) t=t_h+0.2s (d) t=t_h+0.4s

(e) t=t_h+0.6s (f) t=t_h+0.8s

Fig. 7: Isometric views of breaking wave interaction towards the cylinder for different time instant with contour representing the velocity profile in the free surface

distance behind the broken wave crest in Figure 7e.At last, The broken wave appears to spread over the domain and disrupts the incoming waves, as shown in Figure 7f.

The numerically captured free surface elevation probe readings are presented in Figure 10. It allows us to investigate the changes in the free surface elevations during and after the focused wave interaction with the cylinder. To remind the reader, probe WP6 is at the cylinder location, WP5 and WP7 are placed before and after the cylinder location. The numerical results obtained with the Mesh fsM4Co0.1 for WP5 and WP6 replicate the focused wave profile with minor discrepancies in comparison with experiment. The discrepancies are due to the uncertainty produced between the HOS and experimental results and the missing accuracy from the convergence study reported in the previous section. The WP7 displays a considerable difference as the fact that after the cylinder interaction, free surface dynamics are very complex (Figure 7e), and the probe is in the middle of the foam. The numerical probe is subjected to two to three levels of the mixed free surface which cannot record the proper surface elevation irrespective of adequate recording in the physical probe in the experiment.

Next, the focused wave pressure onto the cylinder is evaluated here by comparing the time variation of the dynamic pressure recorded on the submerged as well as exposed surfaces of the cylinder (See Figure 8). The simulated time

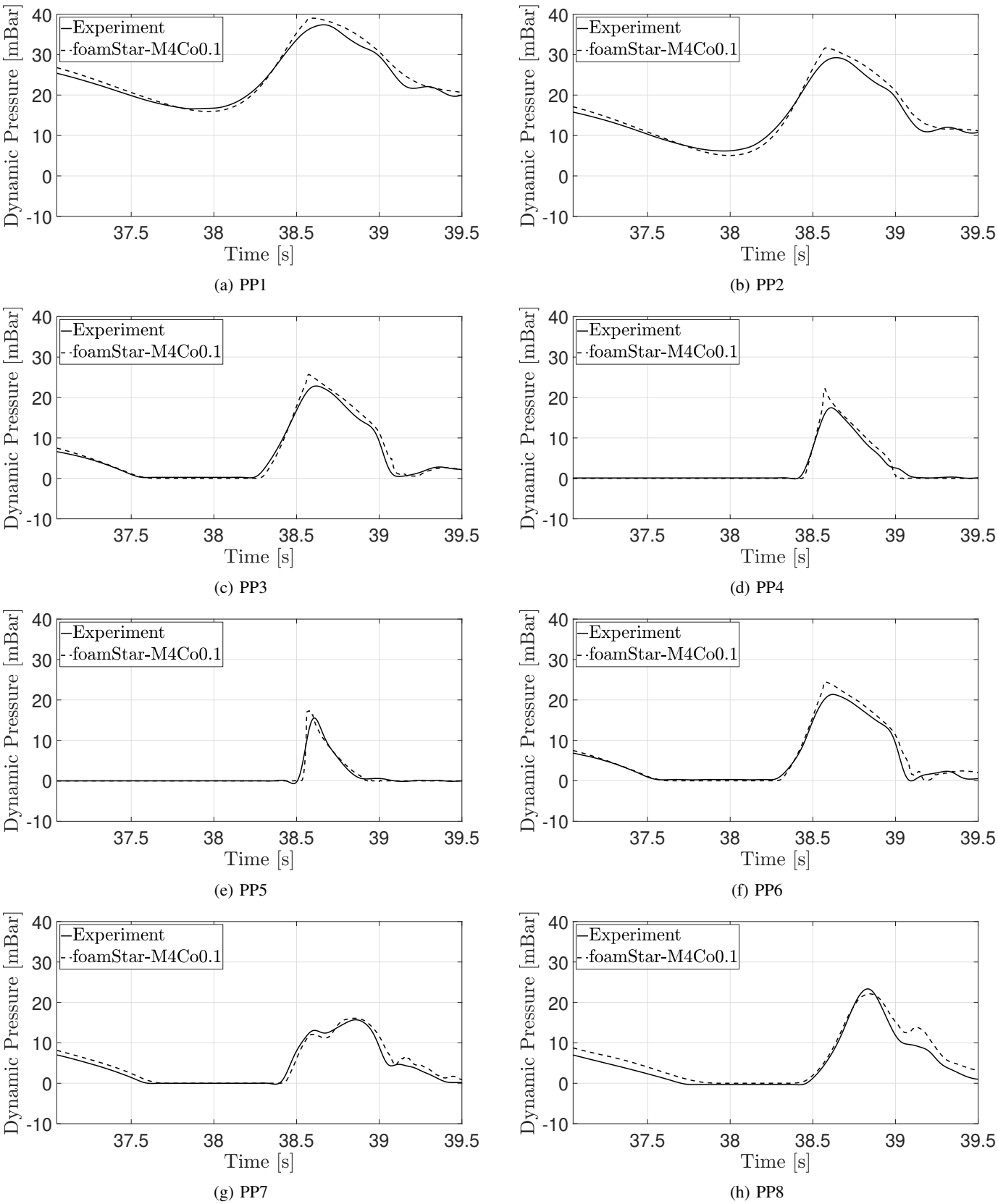

(a) PP1 (b) PP2

(c) PP3 (d) PP4

(e) PP5 (f) PP6

(g) PP7 (h) PP8

Fig. 8: Pressure time history comparison for fixed cylinder in breaking focusing waves between *foamStar* and experiment

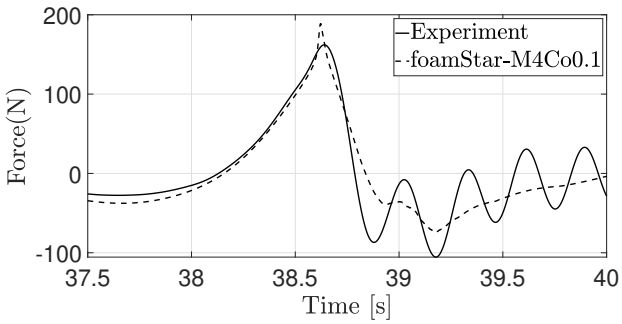

Fig. 9: Comparison of the breaking force between Mesh type fsM4Co0.1 of *foamStar* and experiment

histories of the submerged pressure probes (PP1-PP3) in the stagnation point are expected to follow the wave elevation. Accordingly, the mesh-type fsM4Co0.1 exhibits similar trends, but minor discrepancies are observed. A similar difference exists in simulated peak pressure in PP4 and PP5 (air probes), which depends only on proper wave run-up over the cylinder during the focusing event. Even probes around the cylinder (PP6-8) can capture the trend neatly. The slight deviations in the amplitude of the wave elevation between fsM4Co0.1 and the experiment resulted in the overestimation of pressure amplitudes in almost all the probes.

Figure 9 illustrates the time history of the force recorded for fsM4Co0.1 during the focused wave interaction. In the experiment, the cylinder has experienced the "ringing" phenomenon [33] after impact, which cannot be simulated in numerical simulation as the body is assumed to be rigid. So the time trace is compared only up to impact and ignored the details after the interaction. The hybrid model could represent the breaking force trend accurately but with little overprediction of the force in amplitude. It comes directly from the pressure prediction and the earlier uncertainties mentioned. But assessing the quality of the numerical model shows that it can treat such a complex problem that is of huge importance in ocean engineering at maximum accuracy.

CONCLUSION

The CFD based solver *foamStar*, in coupling with potential theory-based *HOS-NWT* (Domain decomposition Coupling approach), is used to simulate the focused breaking wave interaction with a vertical cylinder. The interaction study is carried as a two-step procedure. First, the focused breaking wave is validated in both the *HOS-NWT* and the *foamStar*. Also, necessary parametric studies are carried out in two dimensional NWT and reported. Second, the breaking wave interaction with the cylinder is carried out. The numerical results for the wave force, the free surface elevation, pressure over the cylinder are compared to the experiment. The experimental data are from tests carried out at the Ludwig-Franzius-Institute, Germany, and obtained an excellent agreement. The highlighted things in the study are the breaking wave model introduced in the potential solver HOS-NWT is tested and the application of domain decomposition methodology for breaking wave interaction problems. The study concludes that this hybrid coupled model as NWT can be a valuable tool for evaluating breaking wave forces over any offshore or coastal structures, replacing the physical tank's difficulties at maximum accuracy.

ACKNOWLEDGEMENT

This work has been performed in the framework of the Chaire Hydrodynamique et Structure Marines CENTRALE NANTES - BUREAU VERITAS. The first author acknowledges IITM and LHEEA, ECN for the financial support for this Ph.D. study.

REFERENCES

[1] V. Sriram, T. Schlurmann, and S. Schimmels, "Focused wave evolution using linear and second order wavemaker theory," *Applied Ocean Research*, vol. 53, pp. 279–296, 2015.

[2] B. M. Sumer and J. Fredsøe, "Scour at the head of a vertical-wall breakwater," *Coastal Engineering*, vol. 29, no. 3-4, pp. 201–230, 1997.

[3] J. Morison, J. Johnson, and S. Schaaf, "The force exerted by surface waves on piles," *Journal of Petroleum Technology*, vol. 2, no. 05, pp. 149–154, 1950.

[4] Y. Goda, "A study on impulsive breaking wave force upon a vertical pile," *Rept. Port and Harbour Res. Inst.*, vol. 5, no. 6, pp. 1–30, 1966.

[5] Ø. Arntsen, X. Ros Collados, and A. Tørum, "Impact forces on a vertical pile from plunging breaking waves," in *Coastal Structures 2011: (In 2 Volumes)*. World Scientific, 2013, pp. 533–544.

[6] J. Wienke and H. Oumeraci, "Breaking wave impact force on a vertical and inclined slender pile—theoretical and large-scale model investigations," *Coastal engineering*, vol. 52, no. 5, pp. 435–462, 2005.

[7] C. Sruthi and V. Sriram, "Wave impact load on jacket structure in intermediate water depth," *Ocean Engineering*, vol. 140, pp. 183–194, 2017.

[8] A. Kamath, M. A. Chella, H. Bihs, and Ø. A. Arntsen, "Breaking wave interaction with a vertical cylinder and the effect of breaker location," *Ocean Engineering*, vol. 128, pp. 105–115, 2016.

[9] V. Sriram, T. Schlurmann, and S. Schimmels, "Focused wave evolution using linear and second order wavemaker theory," *Applied Ocean Research*, vol. 53, pp. 279–296, 2015.

[10] M. Brocchini, "A reasoned overview on boussinesq-type models: the interplay between physics, mathematics and numerics," *Proceedings of the Royal Society A: Mathematical, Physical and Engineering Sciences*, vol. 469, no. 2160, p. 20130496, 2013.

[11] P. Lin and P. L.-F. Liu, "A numerical study of breaking waves in the surf zone," *Journal of fluid mechanics*, vol. 359, pp. 239–264, 1998.

[12] M. A. Chella, H. Bihs, D. Myrhaug, and M. Muskulus, "Breaking characteristics and geometric properties of spilling breakers over slopes," *Coastal Engineering*, vol. 95, pp. 4–19, 2015.

[13] Z. Li, "Two-phase spectral wave explicit navier-stokes equations method for wave-structure interactions," Ph.D. dissertation, Ecole centrale de Nantes, 2018.

[14] C. Lachaume, B. Biausser, P. Fraunié, S. T. Grilli, and S. Guignard, "Modeling of breaking and post-breakingwaves on slopes by coupling of bem and vof methods," in *The Thirteenth International Offshore and Polar Engineering Conference*. OnePetro, 2003.

[15] S. Grilli, R. W. Gilbert, P. Lubin, S. Vincent, D. Astruc, D. Legendre, M. Duval, O. Kimmoun, H. Branger, D. Devrard *et al.*, "Numerical modeling and experiments for solitarywave shoaling and breaking over a sloping beach," in *The Fourteenth International Offshore and Polar Engineering Conference*. OnePetro, 2004.

[16] Y.-M. Choi, Y. J. Kim, B. Bouscasse, S. Seng, L. Gentaz, and P. Ferrant, "Performance of different techniques of generation and absorption of free-surface waves in computational fluid dynamics," *Ocean Engineering*, vol. 214, p. 107575, 2020.

[17] G. Ducrozet, F. Bonnefoy, D. Le Touzé, and P. Ferrant, "A modified high-order spectral method for wavemaker modeling in a numerical wave tank," *European Journal of Mechanics-B/Fluids*, vol. 34, pp. 19–34, 2012.

[18] Y. Choi, B. Bouscasse, S. Seng, G. Ducrozet, L. Gentaz, and P. Ferrant, "Generation of regular and irregular waves in navier-stokes cfd solvers by matching with the nonlinear potential wave solution at the boundaries," in *International Conference on Offshore Mechanics and Arctic Engineering*, vol. 51210. American Society of Mechanical Engineers, 2018, p. V002T08A020.

[19] Z. Li, B. Bouscasse, L. Gentaz, G. Ducrozet, and P. Ferrant, "Progress in coupling potential wave models and two-phase solvers with the swense methodology," in *International Conference on Offshore Mechanics and Arctic Engineering*, vol. 51302. American Society of Mechanical Engineers, 2018, p. V009T13A027.

[20] B. R. Seiffert, G. Ducrozet, and F. Bonnefoy, "Simulation of breaking waves using the high-order spectral method with laboratory experiments: Wave-breaking onset," *Ocean Modelling*, vol. 119, pp. 94–104, 2017.

[21] B. R. Seiffert and G. Ducrozet, "Simulation of breaking waves using the high-order spectral method with laboratory experiments: wave-breaking energy dissipation," *Ocean Dynamics*, vol. 68, no. 1, pp. 65–89, 2018.

[22] C. W. Hirt and B. D. Nichols, "Volume of fluid (vof) method for the dynamics of free boundaries," *Journal of computational physics*, vol. 39, no. 1, pp. 201–225, 1981.

[23] H. Rusche, "Computational fluid dynamics of dispersed two-phase flows at high phase fractions," Ph.D. dissertation, Imperial College London (University of London), 2003.

[24] D. G. Dommermuth, D. K. Yue, W. Lin, R. Rapp, E. Chan, and W. Melville, "Deep-water plunging breakers: a comparison between potential theory and experiments," *Journal of Fluid Mechanics*, vol. 189, pp. 423–442, 1988.

[25] B. J. West, K. A. Brueckner, R. S. Janda, D. M. Milder, and R. L. Milton, "A new numerical method for surface hydrodynamics," *Journal of Geophysical Research: Oceans*, vol. 92, no. C11, pp. 11 803–11 824, 1987.

[26] Z. Tian, M. Perlin, and W. Choi, "An eddy viscosity model for two-dimensional breaking waves and its validation with laboratory experiments," *Physics of Fluids*, vol. 24, no. 3, p. 036601, 2012.

[27] X. Barthelemy, M. Banner, W. Peirson, F. Fedele, M. Allis, and F. Dias, "On a unified breaking onset threshold for gravity waves in deep and intermediate depth water," *Journal of Fluid Mechanics*, vol. 841, pp. 463–488, 2018.

[28] Y. Choi, M. Gouin, G. Ducrozet, B. Bouscasse, and P. Ferrant, "Grid2grid: Hos wrapper program for cfd solvers," *arXiv preprint arXiv:1801.00026*, 2017.

[29] N. G. Jacobsen, D. R. Fuhrman, and J. Fredsøe, "A wave generation toolbox for the open-source CFD library: OpenFoam®," *International Journal for Numerical Methods in Fluids*, vol. 70, no. 9, pp. 1073–1088, 2012.

[30] S. Seng, *Slamming and whipping analysis of ships*. DTU Mechanical Engineering, 2012.

[31] Y. Choi, B. Bouscasse, S. Seng, G. Ducrozet, L. Gentaz, and P. Ferrant, "Generation of Regular and Irregular Waves in Navier-Stokes CFD Solvers by Matching With the Nonlinear Potential Wave Solution at the Boundaries," in *International Conference on Offshore Mechanics and Arctic Engineering*, 06 2018.

[32] V. Sriram, S. Agarwal, S. Yan, Z. Xie, S. Saincher, T. Schlurmann, Q. Ma, T. Stoesser, Y. Zhuang, B. Han *et al.*, "A comparative study on the nonlinear interaction between a focusing wave and cylinder using state-of-the-art solvers: Part a," *International Journal of Offshore and Polar Engineering*, vol. 31, no. 01, pp. 1–10, 2021.

[33] S. Saincher, V. Sriram, S. Agarwal, and T. Schlurmann, "Experimental investigation of hydrodynamic loading induced by regular, steep non-breaking and breaking focused waves on a moving cylinder," *European Journal of Mechanics*, 2022.